

Phase Transition of N -component Superconductors

B. Bergerhoff¹, D. Litim², S. Lola³ and C. Wetterich⁴

Institut für Theoretische Physik
Universität Heidelberg
Philosophenweg 16
69120 Heidelberg, Germany

Abstract

We investigate the phase transition in the three-dimensional abelian Higgs model for N complex scalar fields, using the gauge-invariant average action Γ_k . The dependence of Γ_k on the effective infra-red cut-off k is described by a non-perturbative flow equation. The transition turns out to be first- or second-order, depending on the ratio between scalar and gauge coupling. We look at the fixed points of the theory for various N and compute the critical exponents of the model. Comparison with results from the ϵ -expansion shows a rather poor convergence for $\epsilon = 1$ even for large N . This is in contrast to the surprisingly good results of the ϵ -expansion for pure scalar theories. Our results suggest the existence of a parameter range with a second-order transition for all N , including the case of the superconductor phase transition for $N = 1$.

¹e-mail: bergerho@post.thphys.uni-heidelberg.de

²e-mail: cu9@ix.urz.uni-heidelberg.de

³e-mail: fe6@ix.urz.uni-heidelberg.de

⁴e-mail: wetteric@post.thphys.uni-heidelberg.de

1 Introduction

The quantitative details of the phase transition in superconductors are so far not fully understood. If the phase transition is second-order or very weakly first-order, it is believed that the universal behaviour in the immediate vicinity of the critical temperature can be described by a field theory of electrodynamics with a charged scalar field. Here the scalar field may represent composite degrees of freedom like Cooper-pairs in “standard” superconductors. A non-vanishing expectation value of this scalar field indicates spontaneous symmetry breaking and corresponds to the superconducting phase. Even though the critical behaviour for low temperature superconductors may be difficult to observe, this situation may improve for high temperature superconductors [1]. Also, it is claimed that certain phase transitions in liquid crystals are described by the same universality class as for the superconductors [2]. Critical exponents have been measured for these transitions [3]. An understanding of the critical behaviour in the three-dimensional abelian Higgs model, which should describe all these transitions, is also interesting from the theoretical side: This is the simplest example with a continuous gauge symmetry. Furthermore, the high temperature phase transition in the four-dimensional abelian Higgs model should be well approximated in the vicinity of the phase transition by a three-dimensional effective theory [4]. Here the abelian gauge theory may serve as a prototype for the understanding of the non-abelian model which describes the electroweak phase transition in the early universe.

In this paper we address the problem of the phase transition in the three-dimensional field theory of scalar electrodynamics. Even the order of the phase transition is not settled so far, ranging from proposals of a first-order transition for all values of the coupling constants [5] to speculations about a possible second-order behaviour [6]. On the one side high temperature perturbation theory in the four-dimensional model seems to predict a first-order transition. Perturbation theory is, however, plagued by severe infra-red divergences. In the symmetric phase the one-loop correction to the quartic scalar coupling diverges as k^{-1} , where k is an appropriate infra-red cut-off. Although it is possible to improve the calculations by a resummation of diagrams, there are questions on the reliability of this method [7]. Moreover, from the one-loop correction to the gauge coupling, an infra-red divergence $\sim k^{-1}$ appears if the scalar mass vanishes. Since this is the case approximately near the phase transition, one concludes that in this region the results of perturbation theory will not be accurate. The encountered infra-red problems are exactly those of three-dimensional perturbation theory. In

order to avoid this difficulty an alternative approach uses the ϵ -expansion and attempts to extrapolate results of a computation in $4 - \epsilon$ dimensions to $\epsilon = 1$. This has not given a convincing picture so far. The situation improves somewhat if, in addition, one considers N charged scalar fields with N large. The phase transition is well understood for $N \rightarrow \infty$ but an extrapolation to $N = 1$ is not easy. We will see that even the leading $1/N$ contribution to the critical exponents is not well described by the ϵ -expansion.

In recent years, a new method which deals with these infra-red problems in a non-perturbative way has been proposed [8]. The method is based on the effective average action, Γ_k , for which only fluctuations with momenta $q^2 > k^2$ are included. The scale k acts as an effective infra-red cut-off. An exact, non-perturbative evolution equation describes the scale dependence of the average action [9]. Using this equation, it is possible to follow the k -dependence of Γ_k to extrapolate to the limit $k \rightarrow 0$, where Γ_k becomes the generating functional for the 1PI Green functions. The method has been tested in the Φ^4 -theory [10], where it successfully describes the second-order phase transition that the system undergoes. A study of the critical behaviour of the three-dimensional Φ^4 -theory gives values for the critical exponents in very good agreement with previous estimates [11]. A gauge-invariant effective average action can be constructed for abelian and non-abelian gauge theories [12]. The corresponding non-perturbative exact evolution equation for the abelian Higgs model has been derived for arbitrary dimension d [12]. For $d = 4$ and small gauge coupling, the flow equation is similar to the perturbative renormalization group equations in the one-loop approximation. A numerical study, based on this work, indicates a first-order character for the Coleman-Weinberg phase transition [13], in agreement with the perturbative analysis. However, for $d = 3$, strong renormalisation effects of the gauge coupling result in predictions that may not be obtained by perturbation theory. In particular, the dimensionless coupling e^2 reaches in the scaling limit a value of order $6\pi^2$, thus $e^2/16\pi^2$ is not a small quantity anymore ⁵.

The order of the phase transition seems to depend on the ratio λ_0/e_0^2 of the bare quartic scalar coupling λ_0 and the squared gauge coupling e_0^2 . For small λ_0/e_0^2 (type I superconductors) it was suggested that the phase transition is first-order [5], the discontinuity being induced by fluctuations of the gauge field. This picture has been confirmed by the solution of the non-perturbative flow equation [15]. The question about what happens for large scalar couplings has not found

⁵For the non-abelian Higgs model in three dimensions the dimensionless gauge coupling also grows large. Additional complications arise from confinement effects [14].

a clear answer by previous methods, except for very large N (typically $N \geq 200$) where a second-order phase transition was established for sufficiently large λ_0/e_0^2 . Investigations based on the average action indicate the existence of a range in parameter space where the transition is second-order also for the superconductor ($N = 1$) [15]. If a parameter range for a second-order transition exists for all N there must be a fixed point of the flow equations with associated scale invariant critical behaviour.

In this paper we will use the concept of the average action to examine the critical behaviour of the three-dimensional abelian Higgs model for N complex scalar fields. We will discuss how the fixed points of the theory move as N varies and examine the critical exponents of the model, in the region where a second-order phase transition arises. In section 2 we give a brief sketch of the basic formalism and derive the evolution equations for the running of the couplings. In section 3 we look at the scaling solutions in the large- N approximation. In section 4 we discuss a differential equation which allows us to follow the N -dependence of the fixed points. This uses a linearization of the flow equation for values of the couplings near the fixed point values. In section 5 we give a detailed numerical analysis of the model for various N . The critical exponents for a second-order phase transition are discussed in section 6. In section 7 we present our results and compare them with those obtained through the ϵ -expansion. Finally in section 8 we give a summary of the work and derive the conclusions.

2 Average action and flow equations for running couplings

The starting point of the analysis is the classical action S for N complex scalar fields χ_a , $a = 1, \dots, N$ and the gauge field \mathcal{A}_μ

$$S[\chi, \mathcal{A}_\mu] = \int d^d x \left\{ \frac{1}{4} \mathcal{F}^{\mu\nu} \mathcal{F}_{\mu\nu} + (D^\mu \chi_a)^* (D_\mu \chi^a) - \bar{\mu}^2 \chi_a^* \chi^a + \frac{\bar{\lambda}}{2} (\chi_a^* \chi^a)^2 \right\}, \quad (1)$$

where $\mathcal{F}_{\mu\nu} = \partial_\mu \mathcal{A}_\nu - \partial_\nu \mathcal{A}_\mu$, $D_\mu = \partial_\mu + i\bar{e}\mathcal{A}_\mu$. We note that the pure scalar sector is $O(2N)$ -symmetric. The coupling to the photon reduces this symmetry to $SU(N) \times U(1)$ where the abelian part is gauged. Furthermore, we have the gauge fixing term

$$S_{gf} = -\frac{1}{2\alpha} \int d^d x (\mathcal{A}^\mu - \bar{A}^\mu) \partial_\mu \partial_\nu (\mathcal{A}^\nu - \bar{A}^\nu), \quad (2)$$

where \bar{A}_μ is some arbitrary background field. The average action Γ_k is the effective action for (gauge-invariant) averages of fields. It is obtained by integrating out only quantum fluctuations with (covariant) momenta larger than k . For this purpose one introduces in the functional integral for the usual effective action an infra-red cut-off R_k . If R_k vanishes for $k \rightarrow 0$ one recovers the generating functional for the 1PI Green functions Γ as $\lim_{k \rightarrow 0} \Gamma_k$. The functional $\Gamma_k[\varphi, A]$ is gauge-invariant for all k . The dependence of the effective average action on the scale k is determined by an exact non-perturbative flow equation [12] which reads (up to minor modifications)

$$\frac{\partial}{\partial t} \Gamma_k[\varphi, A] = \frac{1}{2} \text{Tr} \left\{ \left(\frac{\partial R_k[A]}{\partial t} \right) \left(\Gamma_k^{(2)}[\varphi, A] + \Gamma_{gf}^{(2)} + R_k[A] \right)^{-1} \right\} + \frac{\partial}{\partial t} C_k[A]. \quad (3)$$

Here the trace involves a momentum integration and summation over internal indices, $t = \ln k/\Lambda$, and $\Gamma_k^{(2)}$ is the second functional variation of Γ_k . The sum $\Gamma_k^{(2)} + \Gamma_{gf}^{(2)}$ corresponds to the exact inverse propagator in presence of the fields φ and A . We approximate Γ_{gf} by (2) with \mathcal{A}_μ replaced by A_μ . More details can be found in [12] where also the correction $C_k[A]$ is motivated.

The infra-red cut-off R_k acts on scalars ($R_k^{(S)}$) and gauge fields ($R_k^{(G)}$) and reads explicitly

$$\begin{aligned} R_k^{(S)} &= Z_{\varphi,k} \cdot \left(-D^2(A) \right) \frac{f_k^2(-D^2(A))}{1 - f_k^2(-D^2(A))} \\ R_k^{(G)} &= Z_{F,k} \cdot \left(-\partial^2 \right) \frac{f_k^2(-\partial^2)}{1 - f_k^2(-\partial^2)}. \end{aligned} \quad (4)$$

Here $Z_{\varphi,k}$ and $Z_{F,k}$ are appropriate wave function renormalization constants for the scalar and gauge field, respectively. We choose a cut-off that decays exponentially for large (covariant) momentum squared $x = q^2$, i.e.

$$f_k^2(x) = e^{-x/k^2}. \quad (5)$$

For $x \rightarrow 0$ the cut-off $R_k \rightarrow Zk^2$ becomes a mass-like term and suppresses the propagation of quantum fluctuations with $q^2 < k^2$. This eliminates the infra-red-divergence problem that appears in the perturbative approach. For large q^2 the exponential decay of $\partial_t R_k$ guarantees the ultra-violet convergence of the momentum integral in (3). Finally, the use of the covariant derivative in (4) ensures explicit gauge covariance of the flow equation.

A discussion of the phase transition relies mainly on the properties of the effective scalar potential U_k which corresponds to the free energy. In order to extract from (3) the flow equation for the average potential U_k we use a configuration with

$\varphi = \text{const.}$ and $A = 0$. For the derivation of the flow equation for U_k we use a truncation of the average action of the form

$$\Gamma_k[\varphi, A] = \int d^d x \left(\frac{1}{4} Z_{F,k} F_{\mu\nu} F^{\mu\nu} + Z_{\varphi,k} (D^\mu \varphi_a)^* D_\mu \varphi^a + U_k(\rho) \right). \quad (6)$$

The second functional derivative of this expression can be found in appendix A. One obtains for arbitrary dimension d the flow equation

$$\begin{aligned} \frac{\partial}{\partial t} U_k(\rho) &= (d-1)v_d \int dx x^{\frac{d}{2}-1} \tilde{\partial}_t \ln \left(Z_{F,k} P(x) + 2Z_{\varphi,k} \bar{e}^2 \rho \right) \\ &\quad + v_d \int dx x^{\frac{d}{2}-1} \tilde{\partial}_t \ln \left(Z_{\varphi,k} P(x) + U'_k(\rho) + 2\rho U''_k(\rho) \right) \\ &\quad + (2N-1)v_d \int dx x^{\frac{d}{2}-1} \tilde{\partial}_t \ln \left(Z_{\varphi,k} P(x) + U'_k(\rho) \right), \end{aligned} \quad (7)$$

where

$$v_d^{-1} = 2^{d+1} \pi^{d/2} \Gamma\left(\frac{d}{2}\right). \quad (8)$$

Here the potential is a function of the invariant $\rho = \varphi_a^* \varphi^a$ and primes denote derivatives with respect to ρ . We also use the variable $x = q^2$ and the inverse average propagator $P(x)$ is defined by

$$\begin{aligned} ZP(x) &= Zx + R_k(x) \\ P(x) &= \frac{x}{1 - \exp(-\frac{x}{k^2})}. \end{aligned} \quad (9)$$

The partial derivative $\tilde{\partial}_t$ acts only on the infra-red cut-off R_k in P with

$$\tilde{\partial}_t P(x) = k \frac{\partial}{\partial k} P(x) - \left(k \frac{\partial}{\partial k} \ln Z_k \right) (P(x) - x) \quad (10)$$

and we drop the last term proportional to the anomalous dimension in this paper. In the sequel, the use of dimensionless variables turns out to be convenient. We therefore introduce the following variables:

$$u_k(\tilde{\rho}) = k^{-d} U_k(\rho) \quad (11)$$

$$\tilde{\rho} = k^{2-d} Z_{\varphi,k} \rho \quad (12)$$

$$e^2 = k^{d-4} (Z_{F,k})^{-1} \bar{e}^2. \quad (13)$$

In terms of the above, the partial differential equation (7) can be rewritten as

$$\begin{aligned} \partial_t u_k(\tilde{\rho}) &= -d u_k(\tilde{\rho}) + (d-2 + \eta_\varphi) \tilde{\rho} u'_k(\tilde{\rho}) + 2(d-1) v_d l_0^d s_0^d (2e^2 \tilde{\rho}) \\ &\quad + 2(2N-1) v_d l_0^d s_0^d (u'_k(\tilde{\rho})) + 2v_d l_0^d s_0^d (u'_k(\tilde{\rho})) + 2\tilde{\rho} u''_k(\tilde{\rho}), \end{aligned} \quad (14)$$

where primes denote now partial derivatives with respect to $\tilde{\rho}$. The anomalous dimension $\eta_\varphi = -\partial_t \ln Z_{\varphi,k}$ reads

$$\eta_\varphi = -16v_d \left(1 - \frac{1}{d}\right) e^2 l_{1,1}^d(2\lambda\kappa, 2e^2\kappa) + \frac{16}{d} v_d \lambda^2 \kappa m_{2,2}^d(2\lambda\kappa, 0) , \quad (15)$$

and we introduced the dimensionless renormalized vacuum expectation value κ defined through $u'_k(\kappa) = 0$ and the dimensionless renormalized quartic coupling λ as

$$\lambda(k) = u''_k(\kappa(k)) . \quad (16)$$

The constants l_0^d and the threshold functions $s_0^d(\omega)$, $l_{n,m}^d(\omega_1, \omega_2)$ and $m_{n,m}^d(\omega_1, \omega_2)$ are given in appendix B. We also need an evolution equation for $e^2(k)$ that we infer from [12].

The main subject of the present paper is the investigation of solutions to eq. (14). In order to solve eq. (14) for $u_k(\tilde{\rho})$ we make first an Ansatz for the effective potential $u_k(\tilde{\rho})$ as a polynomial expansion around the k -dependent minimum at $\kappa(k)$. The partial differential equation (14) can then be transformed into infinitely many coupled ordinary differential equations for the higher derivatives of the effective potential taken at the vacuum expectation value. To lowest order we find the following coupled set of differential equations for the regime with spontaneous symmetry breaking

$$\begin{aligned} \frac{de^2}{dt} = \beta_{e^2} = & (d-4)e^2 \\ & + \frac{4}{3}v_d e^4 \left[l_g^d \tilde{s}_g^d(2\lambda\kappa, 2e^2\kappa) + l_c^d(2\lambda\kappa) + (N-1)l_{gc}^d \right] \end{aligned} \quad (17)$$

$$\begin{aligned} \frac{d\kappa}{dt} = \beta_\kappa = & (2-d-\eta_\varphi)\kappa + 4\frac{e^2}{\lambda}(d-1)v_d l_1^d s_1^d(2e^2\kappa) \\ & + 6v_d l_1^d s_1^d(2\lambda\kappa) + 2(2N-1)v_d l_1^d \end{aligned} \quad (18)$$

$$\begin{aligned} \frac{d\lambda}{dt} = \beta_\lambda = & (d-4+2\eta_\varphi)\lambda + 8e^4(d-1)v_d l_2^d s_2^d(2e^2\kappa) \\ & + 18\lambda^2 v_d l_2^d s_2^d(2\lambda\kappa) + 2(2N-1)\lambda^2 v_d l_2^d . \end{aligned} \quad (19)$$

The functions $s_n^d(\omega)$, $l_c^d(\omega)$ and $\tilde{s}_g^d(\omega_1, \omega_2)$ describe the threshold effect due to mass terms. They are given, as well as the constants l_n^d , l_{gc}^d and l_g^d , in appendix B. We emphasize that our β -functions are directly computed for arbitrary dimension d and can immediately be evaluated for $d = 3$. No ϵ -expansion around $d = 4$ is necessary. We will see later (sect. 7) that the ϵ -expansion for $\epsilon = 1$ fails to reproduce our results.

The N -dependence in β_κ and β_λ is coming from diagrams that involve the $(2N-1)$ massless scalar modes inside the loop. We note that the scalar contributions are the same as for a pure $SO(2N)$ -symmetric scalar theory for which one has $(2N-1)$ massless Goldstone excitations around a minimum at $\kappa \neq 0$. For β_{e^2} the N -dependence arises from the diagrams that involve the $(N-1)$ fields $\tilde{\sigma}$ and $\tilde{\omega}$ (appendix A). They correspond to $N-1$ complex massless scalars which have a vanishing expectation value. These $2N-2$ real Goldstone modes belong to the fundamental representations of the unbroken global symmetry group $SU(N-1)$. The contribution of the remaining “would be” Goldstone boson (singlet of $SU(N-1)$) is contained in the term for $N=1$.

Starting with sufficiently large initial values of λ/e^2 and solving the system of equations (17)-(19) for $k \rightarrow 0$ shows that κ either runs to zero at some non-vanishing scale k_s or diverges $\sim k^{-1}$. The first behaviour corresponds to the symmetric phase where $\rho_0(k=0) = 0$ whereas the second indicates spontaneous symmetry breaking with $\rho_0(k=0) = \rho_0 > 0$, $\kappa = \rho_0 k^{-1}$. By an appropriate tuning of the initial value of κ the scales k_s or ρ_0 can be made arbitrarily small. The phase transition is second-order. For the initial κ taking exactly the critical value, the solution of the flow equations runs asymptotically towards a scaling solution for $k \rightarrow 0$. This is described by fixed point values κ_* , λ_* and e_*^2 and corresponds to the scale invariant physics at the phase transition. On the other side, for a small ratio of initial values λ/e^2 the coupling λ may reach zero (or extremely small values) for nonvanishing k . Looking at the flow equation (14) for u_k this corresponds to a situation where already the absolute minimum of u_k has jumped to the origin at $\tilde{\rho} = 0$. This behaviour indicates a first-order phase transition.

3 Scaling solutions and large- N approximation

Thus, we find that the abelian Higgs model in three dimensions has a region of parameter values where the phase transition is first-order, and a region where it is second-order. This can be qualitatively understood by looking at the two limits of the theory: When no gauge-field fluctuations are present ($e^2 = 0$) the model reduces to the $2N$ -component Heisenberg model with a second-order phase transition. Below the critical temperature the effective potential U_0 has a maximum at $\rho = 0$ whereas the minimum occurs for $\rho_0 = \rho_0(k=0)$. On the other hand, gauge-field fluctuations dominate the evolution equations for $\lambda \ll e^2$. The solution of the flow equation is then similar to the four-dimensional model [13]

and results in a first-order phase transition. A local minimum remains at the origin even somewhat below the critical temperature.

At the critical temperature T_c of a second-order phase transition the theory becomes scale invariant. This corresponds to a fixed point where the dimensionless parameters κ , λ and e^2 take k -independent values. In consequence, the unrenormalized quantities ρ_0 , $U_k''(\rho_0)$ and \bar{e}^2 vanish with appropriate powers of k . This “second-order fixed point” is infra-red stable in all couplings except one “relevant coupling” that we may associate with κ . We specify short distance (or microscopic) couplings at some appropriate high momentum scale Λ . Then the critical surface, for which the phase transition occurs, is given by a critical value $\kappa_c(\Lambda)$ which is a function of $\lambda(\Lambda)$ and $e^2(\Lambda)$. The difference $\kappa(\Lambda) - \kappa_c(\Lambda)$ is proportional to $T_c - T$. With initial values on the critical surface all couplings flow towards the second-order fixed point if one starts within its range of attraction. This range of attraction also defines the region in parameter space for which the transition is second-order. There must also be a line (more generally a hypersurface) which separates this parameter region from the one for which the transition becomes first-order. On this line, the couplings flow towards another fixed point, the “tricritical fixed point”. This tricritical fixed point has two infra-red unstable directions (in κ and λ). Our picture of a parameter range with second-order transition and a different range with first-order transition is thus realized if two non-trivial fixed points can be identified, one with one and the other with two unstable directions.

We therefore want to investigate the scaling solutions related to the fixed points of the coupled system of differential equations (17) - (19) in three dimensions, i.e. we look for simultaneous zeros of the r.h.s. of eqs. (17) - (19). It turns out that the system (17) - (19) has non-trivial fixed points for any N , although previous results [5], obtained through an ϵ -expansion method, seem to indicate that a large number of complex fields would be needed for this purpose. The main new ingredient for the existence of fixed point solutions even for small N stems from the fact that threshold effects due to the decoupling of massive fluctuations are properly taken into account. As an illustration ⁶, we have depicted in fig. 1 the β -function for λ (19) as a function of λ at fixed $e^2 = e_*^2$. Neglecting the threshold effects corresponds formally to $\kappa = 0$ and results in the upper curve. In this case, no fixed point for λ is obtained. Taking the full threshold behaviour into account (with κ at its fixed point κ_*) reveals the occurrence of two fixed points

⁶We have chosen $N = 10$, but fig. 1 describes the generic behaviour for any N below ~ 183 . For $N > 183$, fixed points are present even when the threshold effects are discarded.

for λ (zeroes for β_λ). Here the smaller value of λ corresponds to the tricritical and the larger one to the second-order fixed point, respectively.

To start a quantitative discussion of the location of the fixed points we consider in this section the large- N limit. The evolution equation for the gauge coupling decouples now completely from the scalar sector and reads

$$\frac{de^2}{dt} = -e^2 + \frac{4}{3}Nv_3l_{gc}^3e^4. \quad (20)$$

Its non-trivial infra-red fixed point solution is given by

$$e_\star^2 = \frac{3}{4v_3l_{gc}^3} \frac{1}{N}. \quad (21)$$

The corresponding solutions for the scalar sector can be obtained through an Ansatz for the large- N behaviour of the couplings as $\kappa \sim N^\alpha$, $\lambda \sim N^\beta$. Inserting this Ansatz in eqs. (18) and (19) it follows that only the pairs

$$(\alpha, \beta) = (1, -1); (1, -2) \quad (22)$$

may yield solutions to the fixed point equation. This result obtains also through an appropriate rescaling of the full partial differential equation (14) and is therefore no mere effect of the polynomial approximation. Here $\lambda_\star \sim 1/N$ corresponds to the second-order fixed point, whereas the tricritical point is characterized by $\lambda_\star \sim 1/N^2$. More explicitly we find for the second-order fixed point ($\beta = -1$) that the influence of the gauge coupling (21) and of the massive scalar fluctuation in the evolution equations (18) - (19) are of subleading order in $1/N$. Therefore, they simplify to

$$\frac{d\kappa}{dt} = -\kappa + 4Nv_3l_1^3 \quad (23)$$

$$\frac{d\lambda}{dt} = -\lambda + 4Nv_3l_2^3\lambda^2, \quad (24)$$

with the corresponding fixed point values given by

$$\kappa_\star = 4v_3l_1^3 N \quad (25)$$

$$\lambda_\star = \frac{1}{4v_3l_2^3} \frac{1}{N}. \quad (26)$$

Since eqs. (20), (23) and (24) are decoupled, it is obvious that the fixed point characterized by eqs. (21),(25) and (26) is infra-red stable in λ and e^2 and unstable

in κ . Since it has only one unstable direction this must be the second-order fixed point. The fixed point values κ_* and λ_* are entirely determined through the fluctuations of the massless modes and any memory of the presence of the gauge field has disappeared in this limit. Therefore, in the large- N limit, the fixed point values λ_* and κ_* are identical to the Wilson-Fisher fixed point of the $O(2N)$ -symmetric pure scalar model. This simple relation does not hold true for the subleading terms in λ_* nor for the critical indices of the theory. The anomalous dimension, for example, reads for the fixed point (21),(25) and (26):

$$\eta_* = \left[\frac{4}{3} \frac{l_1^3}{(l_2^3)^2} m_{2,2}^3(\tilde{m}_*^2, 0) - \frac{8}{l_{gc}^3} l_{1,1}^3(\tilde{m}_*^2, \tilde{M}_*^2) \right] \frac{1}{N}, \quad (27)$$

where \tilde{m}_* (resp. \tilde{M}_*) denotes the dimensionless scalar- (gauge-) field mass at the fixed point:

$$\tilde{m}_*^2 = 2\lambda_*\kappa_* = \frac{2l_1^3}{l_2^3} = 1.7 \quad (28)$$

$$\tilde{M}_*^2 = 2e_*^2\kappa_* = \frac{6l_1^3}{l_{gc}^3} = 6.3. \quad (29)$$

The first term in eq. (27) stems from the scalar fluctuations only (and corresponds to the known result for the pure scalar case), whereas the second term describes the effect of the gauge-field fluctuations. Indeed, the latter one is the dominating term and we find that η_* eq. (27) is negative

$$\eta_* = -\frac{0.31}{N}. \quad (30)$$

Next we turn to the second solution given by $\beta = -2$. Here, the situation changes significantly since eq. (19) simplifies to

$$\frac{d\lambda}{dt} = -\lambda + 16e^4 v_3 l_2^3 s_2^3 (2e^2 \kappa). \quad (31)$$

The fixed point is now given by

$$\lambda_* = 16e_*^4 v_3 l_2^3 s_2^3 (2e_*^2 \kappa_*) = \frac{9l_2^3}{v_3 (l_{gc}^3)^2} s_2^3 (2e_*^2 \kappa_*) \frac{1}{N^2}. \quad (32)$$

In this region, the leading contributions to eq. (31) are coming solely from the gauge-field fluctuations ($\sim 1/N^2$), and even the massless scalar fluctuations contribute only in subleading order ($\sim 1/N^3$). The fixed point (32) is thus a genuine effect of the presence of the gauge field, not present in the pure scalar case. For κ_*

we find a fixed point $\sim N$ which corresponds to the solution of the N -independent implicit equation for $2e_\star^2\kappa_\star$

$$2e_\star^2\kappa_\star = 8v_3l_1^3e_\star^2 \left[N + 2\frac{e_\star^2}{\lambda_\star} s_1^3(2e_\star^2\kappa_\star) \right] = \frac{6l_1^3}{l_{gc}^3} + \frac{l_1^3 s_1^3(2e_\star^2\kappa_\star)}{l_2^3 s_2^3(2e_\star^2\kappa_\star)}. \quad (33)$$

Comparing eq. (29) with eq. (33) we see that the numerical value for κ_\star is affected by corrections from the gauge-field fluctuations. (Remember that the fixed point e_\star^2 eq. (21) is the same for both solutions eq. (22).) We wish to put emphasis on the fact that this fixed point is strictly different from the Gaussian fixed point even in the limit $N \rightarrow \infty$. Analyzing the stability properties of the fixed point specified by (21), (32) and (33) reveals two unstable directions (κ and λ). We associate this point with the tricritical fixed point.

In conclusion, we have found in the large- N approximation two non-trivial fixed point solutions of eqs. (17)-(19). One solution governs the second-order phase transition in this model. The second fixed point is mainly an effect due to the gauge-field fluctuations and governs the tricritical behaviour. Starting, for example, with κ_Λ near $\kappa_c(\Lambda)$, $e_\Lambda^2 = e_\star^2(\Lambda)$ but $\lambda(\Lambda) < \lambda_\star(\Lambda)$ (cf. eq. (32)) the model undergoes a first-order phase transition as $\kappa(\Lambda)$ passes through $\kappa_c(\Lambda)$. Additional fixed points occur for $e_\star^2 = 0$: There is the infra-red unstable Gaussian fixed point at $\lambda_\star = 0$ with κ_\star given by eq. (25) and the Wilson-Fisher fixed point of the pure scalar theory with λ_\star and κ_\star given by (26) and (25). Since $e_\star^2 = 0$ this fixed point is different from the second-order fixed point and has two unstable directions. Finally, if we consider $1/e^4$ instead of e^2 two more similar fixed points exist for $(1/e^4)_\star = 0$. Knowledge of all the fixed points and their stability properties permits easily to establish the qualitative features of the whole phase diagram.

In section 6 we will give a detailed numerical analysis of the second-order fixed point and the tricritical fixed point for arbitrary N . In the same section we will also extend the analysis beyond the very simple approximation (17)-(19) and discuss more elaborate approximations to the flow equation eq. (14).

4 N -dependence of the fixed points

For large N we may obtain the fixed points of the theory by just looking at the leading N -dependent contributions in the beta functions. The N -dependence of the location of the fixed points can be discussed in terms of a simple differential equation which involves the derivatives of the β -functions at the fixed point. A solution of this differential equation, with initial conditions set at large N , allows

to compute the fixed points also for small values of N . In order to derive the flow equation for the N -dependence of the fixed points, we define the generalized vectors

$$\vec{\lambda} = \begin{pmatrix} \kappa \\ \lambda \\ e^2 \end{pmatrix}, \quad \partial_t \vec{\lambda}(N) = \vec{\beta}(\vec{\lambda}(N), N) = \begin{pmatrix} \partial_t \kappa \\ \partial_t \lambda \\ \partial_t e^2 \end{pmatrix}. \quad (34)$$

(This discussion can be easily extended if additional couplings are taken into account). In general, $\vec{\lambda}$ is a function of k and N . However, since we are interested in the scaling solutions for arbitrary N , we wish to take $\vec{\lambda}$ on a fixed point. Therefore, every scale dependence is removed and $\vec{\lambda}$ becomes solely a function of N , $\vec{\lambda}_*(N)$. For all N it obeys the fixed point condition

$$\partial_t \vec{\lambda}_*(N) = \vec{\beta}(\vec{\lambda}_*(N), N) = 0. \quad (35)$$

Taking the total derivative of eq. (35) with respect to N gives the desired differential equation for the N -dependence of $\vec{\lambda}_*$:

$$\frac{\partial \vec{\lambda}_*}{\partial N}(N) = -A^{-1}(\vec{\lambda}_*(N), N) \frac{\partial \vec{\beta}}{\partial N}(\vec{\lambda}_*(N), N). \quad (36)$$

Here, the matrix $A(\vec{\lambda}(N), N)$ is the Hessian matrix at the fixed point,

$$A(\vec{\lambda}, N) = \frac{\partial \vec{\beta}}{\partial \vec{\lambda}}(\vec{\lambda}, N). \quad (37)$$

For given N , it governs the evolution of linearized fluctuations around the scaling solution

$$\partial_t(\vec{\lambda} - \vec{\lambda}_*) = A(\vec{\lambda} - \vec{\lambda}_*). \quad (38)$$

As long as A remains regular, the flow equation (36) has a solution and the fixed point exists for all N in this domain. Also the stability property of the fixed point cannot change in the domain where A remains regular. We have plotted in fig. 2 the eigenvalues of A for the second-order fixed point in dependence on N . All eigenvalues remain far away from zero and depend only moderately on N . Within our truncation we conclude that a second-order fixed point and the associated parameter region for a second-order phase transition exists for arbitrary $N \geq 1$. (This can formally also be continued to $N < 1$). We have numerically solved the flow equation (36), starting initially with large N and extrapolating to $N = 1$. The results that we obtained using this method are in very good agreement with those of the complete numerical analysis that we present in the following section. The difference between the two methods is indistinguishable in the plots.

5 Numerical Analysis

In this section we present in detail the results of a numerical investigation of the fixed-point structure of the abelian Higgs model. Since we are especially interested in the critical behaviour of the theory, we will focus on the existence of fixed point solutions and the related critical indices. As we have mentioned, we employ an expansion around the “asymmetric minimum” at $\kappa \neq 0$, thereby transforming the partial differential equation in an infinite series of coupled ordinary differential equations for the corresponding couplings. This system, then, has to be truncated at some finite order and will be solved numerically.

In lowest approximation, the differential equations are given by eqs. (17) – (19). The numerical values at the second-order fixed point of κ_* , λ_* and e_*^2 are given as functions of the number of complex scalar fields N . Our results are depicted by diamonds in figs. 3-5. The solid lines correspond to the large- N extrapolation as given by eqs. (21), (25) and (26). It turns out that κ_* is very well described by eq. (25) even for $N = 1$. This is related to the fact that the contributions from the massive fluctuations in eq. (18) are damped through the threshold behaviour. The subleading term at $N = 1$ stems from the third term in eq. (18) and is suppressed by a factor of approximately $3s_1^3(2\lambda_*\kappa_*) \sim \mathcal{O}(10^{-2})$ compared to the leading one. The contribution of the gauge-field fluctuation in eq. (18) remains unimportant despite the rather large value for the fixed point of the gauge coupling ($e_*^2 \sim 633$ for $N = 1$). It is suppressed by a factor of $4s_1^3(2e_*^2\kappa_*)e_*^2/\lambda_* \sim \mathcal{O}(10^{-3})$ compared to the leading term. Fig. 4 displays the results for λ_* . Again, we find that λ_* is very well described by its large- N extrapolation eq. (26). Only for $N = 1$ we observe a sizeable correction due to the third term in eq. (19) which becomes nearly of the same order as the last one. Their ratio reads $9s_2^3(2\lambda_*\kappa_*) \sim \mathcal{O}(10^{-1})$ and small corrections are of no surprise. The contribution of the gauge-field fluctuation in eq. (19) is suppressed by a factor of $8s_2^3(2e_*^2\kappa_*)e_*^4/\lambda_*^2 \sim \mathcal{O}(10^{-3})$ and therefore again unimportant. The results for e_*^2 are given in fig. 5. The large- N extrapolation eq. (21) is in a very good agreement with our numerical results down to $N \sim 10$. For $N < 10$, approximating all fluctuations as being massless becomes less and less accurate. The mass of the fluctuations will lower the e^4 -coefficient in eq. (17) as compared to the purely massless estimate and therefore enhance the numerical value for e_*^2 . (Clearly, this effect is largest for $N = 1$ where all contributions in eq. (17) are suppressed by massterms and the estimate eq. (21) becomes too small by roughly a factor of 10.)

In order to check the stability of these findings with respect to a change in the

truncation, we studied approximations of the effective potential being a local polynomial in $(\tilde{\rho} - \kappa)$ up to $(\tilde{\rho} - \kappa)^3$ and $(\tilde{\rho} - \kappa)^4$. (We call these approximations the φ^6 - and φ^8 -approximation, respectively). This approach turned out to be very successful in the pure scalar model [10], where the non-trivial scaling solution corresponds to the Wilson-Fisher fixed point. However, we do not expect that this approach will give reliable results near the tricritical fixed point. Quite generally, the local polynomial approximation around the asymmetric minimum at $\rho_0(k)$ breaks down when $\lambda(k)$ reaches zero for $k > 0$ in the course of its running. This happens near a first-order phase transition and is connected with the fast running of κ and all the higher couplings in the region of very small λ as can be seen from eq. (18). A discontinuity in κ (jumping from $\kappa_c > 0$ to $\kappa = 0$ at $\lambda = 0$) will be manifest through a pole $\sim 1/\lambda$ in the β -functions. Nevertheless, these regions in parameter space can be handled by a more global approach as described in [13] for the $d = 4$ abelian Higgs model. Here, flow equations at the local minimum and at the origin are used simultaneously. At the two extrema we expand in second-order in ρ or $(\rho - \rho_0)$ and guarantee continuity of U_k by assuming a ρ^4 polynomial for the region between 0 and ρ_0 . By this method, the evolution of ρ_0 knows about the flow at the origin (for example the appearance of a new local minimum) and vice versa. As long as U_k exhibits a local asymmetric minimum ($\lambda > 0, \kappa > 0$), the effective average potential is parametrized in terms of the four variables $\lambda, \kappa, m_s^2/k^2$, and λ_s , where $\lambda_s(k) = Z_{\varphi,k}^{-2} U_k''(\rho = 0) k^{-1}$ denotes the dimensionless quartic scalar self-coupling, and $m_s^2(k) = Z_{\varphi,k} U_k'(\rho = 0)$ the scalar mass term at the origin. This second method will serve as an alternative check of the results from the local polynomial approximation at the second-order fixed point in the various approximations. In addition, it will yield results for the tricritical fixed point.

It turns out that κ_* is very stable against changes in the truncation. The results for the φ^6 - and φ^8 -approximation and those obtained with the global method are essentially identical to fig. 3 and differ only slightly from them for small N . The fixed points for e_*^2 and λ_* within the different approximations are depicted in fig. 6. It shows e_*^2 as a function of λ_* for different values of N . The solid line corresponds to the large- N estimate eq. (21) and eq. (26):

$$e_*^2(\lambda_*) = \frac{3l_2^3}{l_{gc}^3} \lambda_* = 3.7 \lambda_* . \quad (39)$$

All the different approximations converge rather fast to the large- N result eq. (39). However, for small values of N the fixed points are quite different. But this has to be expected: The inclusion of a coupling $\sim \varphi^6$ (being dimensionless in $d = 3$) is

for small N an important effect for λ_\star [11]. In turn, e_\star^2 depends now strongly on λ_\star since the massive excitations are important, which results in a sizable shift of the second-order fixed point. On the other side, we do not expect that couplings $\sim \varphi^{10}$ will modify the result of the φ^8 -approximation in an important way. In summary, the second-order fixed point is confirmed in a variety of approximations to the exact evolution equation. The estimates eqs. (21), (25) and (26) give very good predictions already for small N . The results for the critical exponent ν and the anomalous dimension η and their discussion is given in section 7.

Finally, we turn to the tricritical fixed point. In the φ^4 -approximation we find a tricritical point for all $N \geq 2$. For $N = 1$ the gauge coupling runs to infinity in the interesting region and the tricritical point presumably corresponds to $e_\star^2 \rightarrow \infty$. This may well be an artefact of our truncation. Our results obtained by the global approach and the φ^8 -approximation are illustrated in fig. 7. Again, e_\star^2 is given as a function of λ_\star for various values of N . The solid line represents the expected behaviour for large N as given by eq. (21) and eq. (32):

$$e_\star^2(\lambda_\star) \sim \sqrt{\lambda_\star}. \quad (40)$$

This is well reproduced by the global method. Here the results from the φ^8 -approximation converge rather slow to the asymptotic behaviour (40). A comment on the solutions for small N is in order. For $N < 4$ no tricritical fixed point has been found with the global method. This is related to the fact that we have to expand the potential at $\rho = 0$ around a local maximum. The running of the dimensionless mass term at the origin

$$\partial_t \tilde{m}_s^2 = -2\tilde{m}_s^2 - 8v_3 l_1^3 e^2 + \mathcal{O}(\lambda_s, \eta_\varphi \tilde{m}_s^2) \quad (41)$$

is dominated for small N by the e^2 -term. The fixed point for \tilde{m}_s^2 reads therefore

$$(\tilde{m}_s^2)_\star \simeq -4v_3 l_1^3 e_\star^2. \quad (42)$$

Requiring $(\tilde{m}_s^2)_\star$ to stay away from the pole of the threshold functions at $\tilde{m}_s^2 = -1$ yields with the help of eq. (21) the condition

$$N \gtrsim \frac{3l_1^3}{l_{gc}^3} = 3.2, \quad (43)$$

which explains roughly the absence of fixed points for $N \lesssim 4$ in this approach. However, we do not expect this to be a physical effect. Instead, it is related to the

fact that we used in the global approach the evolution equation (17) not only at the asymmetric minimum, but also at the origin. This approximation is harmless in the large- N limit where e_\star^2 (eq. (21)) and the fixed point for the dimensionless renormalized gauge coupling at the origin $e_{0\star}^2$ are both small. Their difference behaves like $1/N$. For small N , in contrast, this may result in a sizeable effect. As a result, $e_{0\star}^2$ is always smaller than e_\star^2 and the bound eq. (43) may therefore be lowered easily.⁷

In conclusion, it has been shown that the second-order and tricritical fixed points are confirmed numerically in a variety of different approximations, locally and globally, to the exact evolution equation (14). The second-order fixed point is shown to be rather stable against higher truncations, especially for large N . For large N we expect a rather fast converge of the series of approximations φ^4 , φ^6 , φ^8 ... towards the scaling solution of the partial differential equation (14) as given by $\partial_t u_k(\tilde{\rho}) = 0$. Since all contributions of terms neglected in the truncation (6) are suppressed by powers of $1/N$, the predictions of critical exponents computed from this fixed point should be very reliable. For small N the convergence of the series of truncations is not obvious with the restricted Ansatz (6). The reason leading to the “missing tricritical point” in the global method will also affect the existence of a scaling solution of eq. (14) and therefore the convergence of the series. For small N it is not excluded that the φ^4 -approximation will give better critical exponents than higher truncations. For the tricritical point the region of convergent truncations is restricted to even higher values of N .

6 Critical exponents

The behaviour of a system near the critical temperature of a second-order phase transition is described by the critical exponents of the theory [16]. These specify the long range correlations of physical quantities as we approach a zero mass theory at $T = T_c$. The system is described by five exponents, which however are not independent. For example the indices γ and δ , which describe the response of the vacuum expectation value ρ_0 to an external magnetic field or source, as well as β , which specifies how the vacuum expectation value depends on the temperature, may be calculated, once both temperature dependence of the correlation length and the behaviour of the connected two-point function at the critical temperature are known. Thus, we will look how the two independent indices ν and η behave

⁷In order to make a full account of this effect, the ρ -dependence of $Z_F(\rho)$ (replacing Z_F in eq. (6)) has to be calculated. We refer this investigation to future work.

as N varies. How these can be computed from properties of the scaling solution is the subject of this section.

The critical exponent η determines the behaviour of the connected two-point function at the critical temperature ($T = T_c$).

$$\lim_{x \rightarrow \infty} \langle \varphi(x)\varphi(0) \rangle_c \sim |x|^{-(d-2+\eta)}. \quad (44)$$

It arises from the anomalous dimension of the field φ and is directly related to the momentum dependence of the (unrenormalized) Green function for $q^2 \rightarrow 0$ at $T = T_c$

$$G^{-1}(q) = q^2 Z(q) \quad (45)$$

$$\lim_{q^2 \rightarrow 0} Z(q) \sim (q^2)^{-\frac{\eta}{2}}. \quad (46)$$

The Green function $G^{-1}(q)$ is encoded in the momentum dependence of the derivative terms in Γ_k which are quadratic in small fluctuations around the $\varphi = \text{const}$ configuration. Its computation goes beyond the truncation (6) and would necessitate a generalization from a constant $Z_{\varphi,k}$ to a momentum dependent function $Z_k(q)$. Then $Z(q)$ in eq. (45) obtains as $\lim_{k \rightarrow 0} Z_k(q)$ whereas $Z_{\varphi,k}$ is given by $\lim_{q^2 \rightarrow 0} Z_k(q)$. Even without computing $Z_k(q)$ explicitly, simple scaling considerations indicate for the critical behaviour

$$Z_k(q) = f\left(\frac{q^2}{k^2}\right) \left(\frac{q^2 + k^2}{\Lambda^2}\right)^{-\frac{\eta}{2}}. \quad (47)$$

Here Λ is some appropriate high momentum scale and the smooth function f approaches constant values for both limits $q^2 \ll k^2$ and $q^2 \gg k^2$. This follows from the observation that q^2 and k^2 act as independent infra-red cut-offs in the loop describing the exact flow equation (3). In consequence, the critical exponent η can be extracted from the k -dependence of the wave function renormalisation for the scaling solution

$$\eta = - \left(\frac{\partial}{\partial t} \ln Z_{\varphi,k} \right)_*. \quad (48)$$

This allows to identify η with η_φ (15), where all couplings are taken at their fixed point values.

We now turn to the critical index ν , which is related to the temperature dependence of the correlation length near the critical temperature T_c

$$\lim_{x \rightarrow \infty} \langle \varphi(x)\varphi(0) \rangle_c \sim e^{-x/\xi}, \quad \xi = m^{-1} \sim |T - T_c|^{-\nu}. \quad (49)$$

Here the renormalized mass m^2 is given by the limit $k \rightarrow 0$ of the k -dependent mass term $m^2(k) = Z_{\varphi,k}^{-1}(k)U'_k(0)$ and $2Z_{\varphi,k}^{-1}U''_k(\rho_0(k))\rho_0(k) = 2\lambda(k)\kappa(k)k^2$, for the symmetric phase and the phase with spontaneous symmetry breaking (SSB), respectively. The phase transition corresponds to a critical trajectory within the SSB regime $m_\star^2(k) = 2\lambda_\star\kappa_\star k^2$.

In order to extract ν we study a small deviation from the critical trajectory

$$m^2(k) = m_\star^2(k) + \delta m^2(k). \quad (50)$$

The evolution equation for δm^2 is characterized by the anomalous mass dimension ω

$$\frac{\partial}{\partial t} \delta m^2 = \omega \delta m^2. \quad (51)$$

For very small $\delta m^2/k^2$ we linearize in δm^2 so that ω becomes independent of δm^2

$$\omega = \frac{\partial \beta_{m^2}}{\partial m^2}(m^2 = m_\star^2) \quad (52)$$

$$\beta_{m^2} = \frac{\partial m^2}{\partial t} = \left(2 + \frac{\beta_\lambda}{\lambda} + \frac{\beta_\kappa}{\kappa}\right)m^2. \quad (53)$$

At the fixed point the anomalous mass dimension is a constant $\omega_\star = \omega_\star(\kappa_\star, \lambda_\star, e_\star^2)$. We therefore obtain in the vicinity of the scaling solution for $\delta m^2 \ll k^2$

$$\delta m^2(k) = \left(\frac{k}{k_1}\right)^{\omega_\star} \delta m^2(k_1). \quad (54)$$

(Here k_1 denotes some scale below the ultra-violet cut-off for which all couplings are near their fixed points. It can be taken proportional to T_c). For $\omega < 2$ the ratio $\delta m^2/k^2$ increases as k becomes smaller. For any non-vanishing $\delta m^2(k_1)$ there is necessarily a critical scale k_c where the linearization of (51) becomes invalid, typically for some constant $c < 1$

$$\delta m_c^2 = \delta m^2(k_c) = ck_c^2. \quad (55)$$

Near the phase transition the renormalized mass is the only scale present. In the SSB phase we conclude from dimensional analysis that it must be proportional to k_c

$$m^2 = m^2(0) = \delta m^2(0) = ak_c^2. \quad (56)$$

The situation is similar in the symmetric phase, but the proportionality constant a is in general different for the symmetric and the SSB phase. We finally observe that $m^2(k_1)$ is a function of temperature and that in linear approximation

$$m^2(k_1, T_c) = m_\star^2(k_1), \quad \delta m^2(k_1) = b(T_c - T). \quad (57)$$

(Remember that the symmetric phase corresponds to $m^2(k_1) < m_\star^2(k_1)$). Combining eqs. (54),(55) and (57) gives

$$k_c^2 = \frac{b}{c} \left(\frac{k_c}{k_1} \right)^{\omega_\star} (T_c - T), \quad (58)$$

and we conclude

$$m^2 = a \left| \frac{b}{c} k_1^{-\omega_\star} \right|^{\frac{2}{2-\omega_\star}} |T - T_c|^{\frac{2}{2-\omega_\star}}. \quad (59)$$

This is to be compared with eq. (49), showing that the critical exponent ν is directly related to ω_\star

$$\nu = \frac{1}{2 - \omega_\star}. \quad (60)$$

We emphasize that (44) with (60) becomes exact in the limit $T \rightarrow T_c$ since the fixed point behaviour completely determines the evolution of m^2 . In other words, the “initial” and “final” running of m^2 away from the fixed point becomes negligible compared to the running near the fixed point. The preceding discussion has been explicitly verified by numerical studies for the pure scalar theory [10]. We still have to specify how the anomalous mass dimension ω_\star should be evaluated. In fact the ratios $\frac{\beta_\lambda}{\lambda}$ and $\frac{\beta_\kappa}{\kappa}$ in eq. (53) depend not only on $\lambda\kappa$ or m^2 which we have up to now taken as a variable for simplicity of the presentation. They also involve λ and e^2 (and in principle also some other parameters characterizing the average action, like for example the φ^6 coupling). For a computation of ω_\star we have to specify how the couplings we are using depend on each other. Instead of

m^2 we use here κ as the independent parameter and express λ and e^2 as a function of κ . (This can easily be extended if additional couplings are considered). Then ω_* can be expressed in terms of the partial derivatives of β_κ evaluated at the fixed point:

$$\omega_* = 2 + \left(\frac{\partial \beta_\kappa}{\partial \kappa} \right)_* + \frac{\partial \lambda}{\partial \kappa} \left(\frac{\partial \beta_\kappa}{\partial \lambda} \right)_* + \frac{\partial e^2}{\partial \kappa} \left(\frac{\partial \beta_\kappa}{\partial e^2} \right)_*. \quad (61)$$

It remains a determination of the quantities $\frac{\partial \lambda(\kappa)}{\partial \kappa}$ and $\frac{\partial e^2(\kappa)}{\partial \kappa}$. The phase transition ($T = T_c$) corresponds to a running along a trajectory on the critical surface into the second-order fixed point. Trajectories infinitesimally close to the critical surface (for T infinitesimally close to T_c) come infinitesimally close to the fixed point and then move away from it infinitesimally close to a curve denoted as “unstable direction”. The dependence $\lambda(\kappa)$ and $e^2(\kappa)$ on the curve corresponding to the unstable direction should be used in the equation for ω_* . More formally, the evolution equation for small deviations from the fixed point

$$\delta \kappa = \kappa - \kappa_*, \quad \delta \lambda = \lambda - \lambda_*, \quad \delta e^2 = e^2 - e_*^2 \quad (62)$$

can be written as

$$\frac{\partial}{\partial t} \begin{pmatrix} \delta \kappa \\ \delta \lambda \\ \delta e^2 \end{pmatrix} = A \begin{pmatrix} \delta \kappa \\ \delta \lambda \\ \delta e^2 \end{pmatrix} \quad (63)$$

with (cf. sect. 4)

$$A = \begin{pmatrix} \partial \beta_\kappa / \partial \kappa & \partial \beta_\kappa / \partial \lambda & \partial \beta_\kappa / \partial e^2 \\ \partial \beta_\lambda / \partial \kappa & \partial \beta_\lambda / \partial \lambda & \partial \beta_\lambda / \partial e^2 \\ \partial \beta_{e^2} / \partial \kappa & \partial \beta_{e^2} / \partial \lambda & \partial \beta_{e^2} / \partial e^2 \end{pmatrix}. \quad (64)$$

At the second-order fixed point all eigenvalues of the matrix A , except one, are positive. Let us denote by $x^{us} = (1, b_2, b_3)$ the eigenvector corresponding to the negative eigenvalue. As k decreases, only this eigenvector plays a role. It indicates the unstable direction whereas the components corresponding to positive eigenvalues quickly die out. For the unstable direction we therefore find that $\frac{\lambda}{\kappa} = b_2$, or, for the equation for ω_* , $\frac{\partial \lambda}{\partial \kappa} = b_2$, $\frac{\partial e^2}{\partial \kappa} = b_3$. Since in general A is not a symmetric matrix, we should specify what we mean by an eigenvector. We denote by θ the unique, negative eigenvalue of A . Using the transformation

$\tilde{A} = C^{-1}AC$ we can bring \tilde{A} to a form where $\tilde{A}_{i1} = \theta\delta_{i1}$. Then the unstable direction corresponds to the vector

$$\tilde{x}_i^{us} = C_{ij}^{-1}x_j^{us} = c\delta_{i1} \quad (65)$$

with

$$\frac{\partial}{\partial t}\tilde{x}^{us} = \theta\tilde{x}^{us}. \quad (66)$$

Inverting (65) we can read off $b_i = \frac{C_{i1}}{C_{11}}$ where the coefficients C_{i1} obey $A_{ij}C_{j1} = \theta C_{i1}$. This completely specifies ω_* by the derivatives of the β -functions at the fixed point. Knowledge of the fixed point values of the couplings for arbitrary N and the corresponding β -functions provides the value of ν by simple algebraic manipulations.

7 Results and comparison with ϵ -expansions

In this section, we compare our results for the critical indices at the second-order phase transition with those obtained earlier by other authors for large values of N . Our numerical results are given in figs. 8 and 9 for the anomalous dimension η and the critical index ν , respectively. Different methods have been tried in the past to compute these critical exponents for large N [5, 17]. Since all methods (including ours) are thought to give the most accurate values for large N , a comparison of the results is best made for $N \rightarrow \infty$ where $\eta \sim \frac{1}{N}$ and $\nu - 1 \sim \frac{1}{N}$. In table 1 we compare the coefficients $N\eta(N)$ and $N(\nu(N) - 1)$ as obtained by various methods. In our approach the different approximations (and the global method) converge very well for these quantities in the large- N limit. Our result of the anomalous dimension is given by eq. (27). We have not computed an analytical expression for the subleading coefficient of ν . This would require a systematic expansion of the quantities appearing in the last section in powers of $1/N$. However, this coefficient has been obtained by a numerical fit of the data for $\nu(N)$ to a polynomial in $1/N$ and we find $\nu = 1 - \frac{1.38}{N}$.

Two papers quote results of a large- N estimate from a computation in fixed dimension $d = 3$. We should emphasize here that the situation for a gauge theory is rather different from the pure $2N$ -component scalar theory where exact large- N results can be obtained. A loop computation in three dimensions requires the presence of an effective infra-red cut-off for all fields. In the pure scalar theory this

The limit $N \rightarrow \infty$ of	$N\eta(N)$	$N[\nu(N) - 1]$
Our result:	-0.31	-1.38
Previous large- N estimates [5, 17]:	-2.03	-4.86
ϵ -expansion at $\epsilon = 1$ around		
a) $d = 4 - \epsilon$ [5]:	$-9 + \mathcal{O}(\epsilon^2)$	$-48 + \mathcal{O}(\epsilon^2)$
b) $d = 2 + \epsilon$, CP^{N-1} model, order ϵ^2 [17]:		$-2 + \mathcal{O}(\epsilon^3)$
c) $d = 2 + \epsilon$, CP^{N-1} model, order ϵ^4 [17]:		$-6 + \mathcal{O}(\epsilon^5)$

Table 1

is provided by the scalar mass term if the phase transition is approached from the symmetric phase [18]. For the gauge model investigated here the photon remains massless in the symmetric phase and produces an infra-red divergence in the loop expansion. This problem persists in the large- N approximation. Thus perturbative calculations in three dimensions have to introduce some infra-red cut-off by hand. We give the estimate of such methods [5, 17] in table 1. In our approach, the infra-red cut-off is always provided by the averaging scale k and no additional assumptions have to be made. We find a substantial discrepancy of previous large- N estimates from our result for $d = 3$. Nevertheless, we expect that the relatively crude estimates of ref. [5, 17] give rather realistic results for $d \approx 4$ and $d \approx 2$. For $d = 4$ the infra-red divergence is only logarithmic and the exact form of the infra-red cut-off does not matter. For $d = 2$ there are no transverse photon degrees of freedom and the infra-red problem in the loop expansion may be circumvented.

As an alternative to fixed dimension large- N estimates one may attempt to use an extrapolation of results in $4 - \epsilon$ dimensions to $\epsilon = 1$ (ϵ -expansion) [5, 19]. Results of this method for the critical exponents are also shown in table 1. We emphasize that the result in order ϵ differs from our result by factors of about 30 for both $N\eta$ and $N(\nu - 1)$! These rather large differences can directly be traced to the threshold effects for the massive fluctuations which are neglected in lowest order ϵ -expansion. This can be seen by neglecting the masses in eq. (27): The leading $1/N$ coefficient in the anomalous dimension would then reach -9.53 and be of the same order as the ϵ -expansion result -9 . For $d \rightarrow 4$ ($\epsilon \rightarrow 0$) the mass terms are small at the fixed point and the ϵ -expansion becomes reliable. For $d = 3$, however, the mass terms are substantial and the ϵ -expansion fails to reproduce the leading $1/N$ coefficient correctly. This is directly related to the absence of a second-order fixed point for moderate values of N within the lowest order ϵ -approximation. In contrast to the $O(N)$ symmetric pure scalar theory,

N	$\eta(\varphi^4)$	$\eta(\varphi^8)$	$\nu(\varphi^4)$	$\nu(\varphi^8)$
1	-0.134	-0.170	0.532	0.583
2	-0.0892	-0.123	0.639	0.568
3	-0.0672	-0.0835	0.715	0.664
5	-0.0453	-0.0513	0.798	0.777
7	-0.0343	-0.0374	0.843	0.832
10	-0.0252	-0.0267	0.883	0.877
30	-0.00909	-0.00926	0.956	0.956
100	-0.00281	-0.00283	0.986	0.986

Table 2

where the ϵ -expansion gives very good estimates for the critical exponents [20], we conclude that the ϵ -expansion gives a very misleading picture of the nature of the phase transition for small values of N and sufficiently large λ/e^2 .

Finally, in the limit $e^2 \rightarrow \infty$ the N -component abelian Higgs model is thought to be described by a pure scalar CP^{N-1} model [21]. We notice that towards the infra-red $e^2(k)$ decreases very fast for large N . The effect of $1/e^2 \neq 0$ corresponds therefore to a relevant parameter in the appropriately perturbed CP^{N-1} model. Nevertheless, if $e_*^2 \kappa_*$ remains very large at the true second-order fixed point of the abelian Higgs model, the critical exponents may be close to the ones of the CP^{N-1} model. The critical exponents of the CP^{N-1} model have been computed by an expansion around $2 + \epsilon$ dimensions up to order ϵ^4 [17]. We notice a rather poor convergence of the ϵ -series for large N and $\epsilon = 1$. The quoted values of the leading $1/N$ coefficients are also tabulated in table 1 and turn out to be much larger than our results. At this stage it is not clear if this is a failure of the ϵ -expansion for the CP^{N-1} model, or if the $1/N$ coefficients of the critical exponents in the abelian Higgs model differ substantially from the ones of the CP^{N-1} model.

Let us next turn to small values of N . The rather small values of the $1/N$ -coefficients of η and $\nu - 1$ allow a rather smooth extrapolation towards small N (cf. figs. 8 and 9). This is in contrast to previous computations. In order to see the effects of the approximations we have depicted in figs. 8 and 9 solutions of two different approximations to eq. (14). For $N > 10$ their difference is negligible. However, for $N < 10$, effects of higher couplings begin to have a sizeable influence on the critical exponents η and ν . As discussed briefly in sect. 5, we do not expect a good convergence of the truncation series for small N . This is also apparent

from our results for $N \leq 2$. The most reliable estimate at present is probably the one of the φ^4 -approximation.

In table 2, we give the critical indices of the second-order phase transition for different values of N and for different approximations. We notice that for all values of N the anomalous dimension turns out negative. This is in contrast to pure $O(N)$ -symmetric scalar theories and is due to the gauge field fluctuations. Since for $N = 2$ the CP^1 model is equivalent to an $SO(3)$ model which has positive η we conclude that for small N our critical exponents differ substantially from the CP^{N-1} model. It is also clear that the critical exponents deviate from the $O(2N)$ scalar theory which is obtained for $e^2 = 0$. This is true for all N .

8 Conclusions

We have presented a non-perturbative analysis of the scaling behaviour of the three-dimensional abelian Higgs model for N complex scalar fields. It is based on the investigation of fixed points of non-perturbative flow equations which describe the scale dependence of the average action. One fixed point governs the second-order phase transition (for the appropriate parameter range) whereas the other corresponds to the tricritical point where the second-order transition changes to a first-order one. We have found a second-order fixed point for all values of N , including the case of the superconductor for $N = 1$ ⁸. This suggests a second-order phase transition for type II superconductors with sufficiently strong scalar coupling. Such a picture is consistent with lattice studies⁹ [22]. We have computed the critical exponents η and ν in dependence on N . For $N = 1$ we obtain η between -0.13 and -0.17 and ν between 0.53 and 0.58 . From the scaling laws we infer α between 0.25 and 0.4 , β between 0.23 and 0.24 and γ between 1.254 and 1.135 . The phase transition from nematic to smectic-A in liquid crystals is thought to be modeled by the same universality class as superconductors. Our values for the critical exponents may therefore be compared to the measured values for the transition in these liquid crystals. The indices α and γ agree within the experimental uncertainties. For ν the experiment distinguishes between parallel and perpendicular directions [3], and direct comparison with our value is more difficult.

We find a very smooth transition between the behaviour for large and small N . In

⁸The case $N = 1$ is studied in full detail in ref. [15].

⁹Lattice studies cannot distinguish between a second-order and a weakly first-order transition.

particular, the $1/N$ -expansion seems to remain valid down to rather small values of N . We were also able to find the tricritical fixed point, even though our global method could not be used for $N < 4$. We have not attempted here to compute the crossover exponents associated to this fixed point. This can be done by methods in complete analogy to sect. 6. We expect our results for the tricritical fixed point to be less reliable than the ones for the second-order fixed point. This is connected to shortcomings of the present truncation that will be discussed below. An important message from the present work concerns the validity of the ϵ -expansion. In contrast to $O(N)$ -symmetric scalar theories we find that the ϵ -expansion gives for all N a rather poor description of the phase transition in the three-dimensional abelian Higgs model. For large N the ϵ -expansion results for the leading $1/N$ coefficients of η and $\nu - 1$ are off by a factor of 30. For low N the ϵ -expansion would suggest a first-order transition for all parameter values, in contrast to our findings.

Let us finally discuss the limits of quantitative validity of our results. This mainly concerns the truncation (6) which leads to the non-perturbative flow equations (14), (15) and (17). This truncation can be viewed as a lowest order approximation of a systematic derivative expansion of the most general form of the average action Γ_k . The next order should replace the coefficient $Z_{F,k}$ in eq. (6) by a function $Z_{F,k}(\rho)$ and similar for the scalar kinetic terms. This will lead to additional contributions to the flow equations for the potential and the anomalous dimension η_φ which involve ρ -derivatives like Z' [8, 11]. The most important modification, however, is probably the effective replacement of e^2 by a ρ -dependent function. Furthermore, it may become necessary to take the effective momentum dependence of e^2 into account. All this can be done by exploiting the exact flow equation with less severe truncations. In the present truncation, eq. (6), the treatment of the region around the origin ($\rho = 0$) seems not very reliable in the SSB regime where the potential minimum occurs for $\rho_0 \neq 0$. In particular, we use at the origin effectively $e^2(\rho_0)$ instead of $e^2(0)$. The resulting errors are particularly important for small N and we believe that this is the reason why we did not find the tricritical fixed point with the global method for $N < 4$. Similarly, it seems probable that no exact scaling solution exists for the full system of flow equations (14), (15) and (17) for small N [23]. Since the problem appears to be mainly related to the behaviour at the origin, a local approximation (in ρ) seems more appropriate at the moment for the treatment of the second-order fixed point. A definite computation of the parameter range where the phase transition in superconductors is second-order requires an understanding of the mentioned truncation problems and the demonstration of a fully scale invariant solution for $u_k(\tilde{\rho})$.

Appendices

A Functional derivative of the average action

For the derivation of the second functional derivative $\Gamma_k^{(2)}$, evaluated at $\varphi_a = \sqrt{\rho}\delta_{a1}$ and arbitrary A_μ we make the following decomposition [12] of the fluctuations $\delta\varphi$, δA :

$$\begin{aligned}\delta A_\mu &= t_\mu + \sqrt{\alpha} \frac{\partial_\mu}{\sqrt{-\partial^2}} \tilde{\ell}, \quad \partial^\mu t_\mu = 0 \\ \delta\varphi_1 &= \frac{1}{\sqrt{2}} (\sigma + i\omega) \\ \delta\varphi_a &= \frac{1}{\sqrt{2}} (\tilde{\sigma}_a + i\tilde{\omega}_a), \quad a > 1.\end{aligned}\tag{67}$$

Concerning the scalar sector we observe one massive mode σ , one massless Goldstone mode ω and $2(N-1)$ massless pseudo-Goldstone bosons $\tilde{\sigma}_a$, $\tilde{\omega}_a$, $a > 1$. Working in the Landau gauge ($\alpha = 0$) one finds

$$\begin{aligned}\int d^d x \delta\psi \tilde{\Gamma}^{(2)} \delta\psi &= \int d^d x \left\{ t_\mu [Z_{F,k} P(-\partial^2) + 2\bar{e}^2 Z_{\varphi,k\rho}] t^\mu \right. \\ &\quad + \tilde{\ell} P(-\partial^2) \tilde{\ell} + \sigma [Z_{\varphi,k} P(-D^2)_{sy} + U'_k + 2\rho U''_k] \sigma \\ &\quad + \omega [Z_{\varphi,k} P(-D^2)_{sy} + U'_k] \omega + 4\sqrt{2}\bar{e}^2 \sqrt{\rho} Z_{\varphi,k} t_\mu A^\mu \sigma \\ &\quad + 2Z_{\varphi,k} \omega P(-D^2)_{as} \sigma \\ &\quad + \sum_{a=2}^N \left(\tilde{\sigma}_a [Z_{\varphi,k} P(-D^2)_{sy} + U'_k] \tilde{\sigma}_a \right. \\ &\quad + \tilde{\omega}_a [Z_{\varphi,k} P(-D^2)_{sy} + U'_k] \tilde{\omega}_a \\ &\quad \left. \left. + 2Z_{\varphi,k} \tilde{\omega}_a P(-D^2)_{as} \tilde{\sigma}_a \right) \right\},\end{aligned}\tag{68}$$

where

$$F[A]_{sy} = \frac{1}{2} (F[A] + F[-A]), \quad F[A]_{as} = \frac{1}{2i} (F[A] - F[-A]).\tag{69}$$

Putting $A_\mu = 0$ ($D^2 = \partial^2$) and switching to momentum space, yields $\Gamma_k^{(2)}[\varphi, 0]$ as needed for the derivation of the flow equation (7) for the average potential.

B Threshold functions and constants

We use the following threshold functions and constants:

$$l_0^d = \frac{1}{2} k^{-d} \int_0^\infty dx x^{\frac{d}{2}-1} \tilde{\partial}_t \ln(P(x))$$

$$\begin{aligned}
l_{n \geq 1}^d &= -\frac{1}{2} k^{2n-d} \int_0^\infty dx x^{\frac{d}{2}-1} \tilde{\partial}_t P(x)^{-n} \\
l_g^{d \geq 3} &= -\frac{d-2}{4} k^{4-d} \int_0^\infty dx x^{\frac{d}{2}-2} \frac{d}{dx} \left[\frac{1}{P(x)} \tilde{\partial}_t P(x) \right] \\
s_0^d(\omega) &= \frac{1}{2l_0^d} k^{-d} \int_0^\infty dx x^{\frac{d}{2}-1} \tilde{\partial}_t \ln(P(x) + \omega k^2) \\
s_{n \geq 1}^d(\omega) &= -\frac{1}{2l_n^d} k^{2n-d} \int_0^\infty dx x^{\frac{d}{2}-1} \tilde{\partial}_t (P(x) + \omega k^2)^{-n} \\
l_{n,m}^d(\omega_1, \omega_2) &= -\frac{1}{2} k^{2(n+m)-d} \int_0^\infty dx x^{\frac{d}{2}-1} \times \\
&\quad \tilde{\partial}_t \left[(P(x) + \omega_1 k^2)^{-n} (P(x) + \omega_2 k^2)^{-m} \right] \\
m_{n,m}^d(\omega_1, \omega_2) &= -\frac{1}{2} k^{2(n+m-1)-d} \int_0^\infty dx x^{\frac{d}{2}} \times \\
&\quad \tilde{\partial}_t \left[\left(\frac{dP}{dx} \right)^2 (P(x) + \omega_1 k^2)^{-n} (P(x) + \omega_2 k^2)^{-m} \right] \\
n_{n,m}^d(\omega_1, \omega_2) &= -\frac{1}{2} k^{2(n+m-1)-d} \int_0^\infty dx x^{\frac{d}{2}} \times \\
&\quad \tilde{\partial}_t \left[\frac{dP}{dx} (P(x) + \omega_1 k^2)^{-n} (P(x) + \omega_2 k^2)^{-m} \right] \\
l_c^{d \geq 3}(\omega) &= \frac{d-2}{4} k^{4-d} \int_0^\infty dx x^{\frac{d}{2}-2} \frac{d}{dx} \frac{d}{dt} \ln \left(1 + \frac{P(x) - x}{k^2(1 + \omega)} \right) \\
l_{gc}^d &= l_g^d + l_c^d(0). \tag{70}
\end{aligned}$$

Here $\tilde{\partial}_t$ stands for $\frac{\partial}{\partial t}$ acting only on R_k contained implicitly in $P(x)$ (see sect. 2). These functions, as well as expressions for the asymptotic behaviour of $s_n^d(\omega)$ for $\omega \rightarrow \infty$ can be found in [11]. In terms of the above, the threshold function from the massive fluctuations for β_{e^2} in eq. (17) reads

$$\begin{aligned}
\tilde{s}_g^d(2\lambda\kappa, 2e^2\kappa) &= \frac{48e^2\kappa}{d(d+2)l_g^d} \left[(d+1)m_{2,2}^d(2\lambda\kappa, 2e^2\kappa) - n_{2,1}^{d-2}(2\lambda\kappa, 2e^2\kappa) \right] \\
&\quad + \frac{m_{2,2}^{d+2}(2\lambda\kappa, 0)}{m_{2,2}^{d+2}(0, 0)}. \tag{71}
\end{aligned}$$

Furthermore, for large mass terms $\omega_2 \gg 1$ we have

$$\begin{aligned}
\lim_{\omega_2 \rightarrow \infty} l_{n,m}^d(\omega_1, \omega_2) &= l_n^d s_n^d(\omega_1) \omega_2^{-m} + \mathcal{O}(\omega_2^{-(m+1)}) \\
\lim_{\omega_2 \rightarrow \infty} m_{n,m}^d(\omega_1, \omega_2) &= m_{n,0}^d(\omega_1, 0) \omega_2^{-m} + \mathcal{O}(\omega_2^{-(m+1)}) \\
\lim_{\omega_2 \rightarrow \infty} n_{n,m}^d(\omega_1, \omega_2) &= n_{n,0}^d(\omega_1, 0) \omega_2^{-m} + \mathcal{O}(\omega_2^{-(m+1)}). \tag{72}
\end{aligned}$$

References

- [1] M. B. Salomon et al, Physica **A200** (1993), 365.
- [2] B. I. Halperin and T. C. Lubensky, Solid State Commun. **14** (1974), 997;
P. G. De Gennes, Solid State Commun. **14** (1974), 997.
- [3] D. L. Johnson et al, Phys. Rev. **B18** (1978), 4902;
C. W. Garland, G. B. Kasting and K. J. Lushington, Phys. Rev. Lett **43**
(1979), 1420;
C. W. Garland et al, Phys. Rev. **A27** (1983), 3234;
J. Thoen, H. Marynissen and W. Van Daal, Phys. Rev. Lett **52** (1984), 204;
B. M. Ocko, R. J. Birgeneau, J. D. Litster and M. E. Neubert, Phys. Rev. Lett.
52 (1984), 208.
- [4] S. Weinberg, Phys. Lett. **B91** (1980), 51;
T. Appelquist and R. Pisarski, Phys. Rev. **D23** (1982), 2305;
S. Nadkarni, Phys. Rev. **D27** (1983), 917;
N. P. Landsman, Nucl. Phys. **B322** (1989), 498.
- [5] B. I. Halperin, T. C. Lubensky and S. Ma, Phys. Rev. Lett. **32** (1974), 292.
- [6] C. Dasgupta and B. I. Halperin, Phys. Rev. Lett. **47** (1981), 1556;
H. Kleinert, Lett. Nuov. Cim. **25** (1982), 405;
J. March-Russell, Phys. Lett. **B296** (1992), 364.
- [7] J. R. Espinosa, M. Quiros and F. Zwirner, Phys. Lett. **B314** (1993), 206;
W. Buchmüller, Z. Fodor, T. Helbig and D. Walliser, Ann. Phys. **234** (1994),
260;
D. Bödeker, W. Buchmüller, Z. Fodor and T. Helbig, Nucl. Phys. **B423**
(1994), 171.
- [8] C. Wetterich, Nucl. Phys. **B352** (1991), 529;
C. Wetterich, Z. Phys. **C57** (1993), 451; **C60** (1993), 461.
- [9] C. Wetterich, Phys. Lett. **B301** (1993), 90.
- [10] N. Tetradis and C. Wetterich, Nucl. Phys. **B398** (1993), 659.
- [11] N. Tetradis and C. Wetterich, Nucl. Phys. **B422** (1994), 541.
- [12] M. Reuter and C. Wetterich, Nucl. Phys. **B408** (1993), 91; **B417** (1994),
181; **B427** (1994), 291.

- [13] D. Litim, C. Wetterich and N. Tetradis, HD-THEP-94-23 and OUTP-94-12 preprint.
- [14] B. Bergerhoff and C. Wetterich, HD-THEP-94-31 preprint.
- [15] B. Bergerhoff et. al., “Phase diagram of superconductors”, HD-THEP-95-5 preprint.
- [16] See e.g. D. J. Amit, *Field Theory, the Renormalization Group, and Critical Phenomena*, World Scientific, 1984.
- [17] S. Hikami, Prog. Theor. Phys. **62**, No. 1 (1979), 226.
- [18] G. Parisi, J. Stat. Phys. **23** (1980), 49; *Statistical Field Theory*, Addison Wesley, 1988.
- [19] P. Arnold and L. Yaffe, Phys. Rev. **D49** (1994), 3003.
- [20] See e.g. J. Zinn-Justin, *Quantum Field Theory and Critical Phenomena*, Oxford Science Publications, 1989.
- [21] M. Lüscher, Phys. Lett. **B78** (1978), 465;
E. Witten, Nucl. Phys. **B149** (1979), 285.
- [22] J. Bartholomew, Phys. Rev. **B28** (1983), 5378;
Y. Munehisa, Phys. Lett. **B155** (1985), 159.
- [23] N. Tetradis, private communication.

Figure captions

- Fig. 1: The β_λ -function eq. (19) is given in dependence on λ for $N = 10$ and two values of κ . The arrows indicate the flow with scale $k \rightarrow 0$. No fixed points are obtained when the threshold behaviour is discarded, $\kappa = 0$ (upper curve, right axis). In contrast, the inclusion of the threshold effects with $\kappa = \kappa_*$ allows for two fixed points (lower curve, left axis).
- Fig. 2: Eigenvalues of the fluctuation matrix A in dependence on N . The two positive eigenvalues indicate that the fixed point corresponds to a second-order phase transition for all N .
- Fig. 3: Fixed point value κ_* in dependence on N for a φ^4 -approximation.
- Fig. 4: Fixed point value λ_* in dependence on N for a φ^4 -approximation.
- Fig. 5: Fixed point value e_*^2 in dependence on N for a φ^4 -approximation.
- Fig. 6: Values for e^2 and λ at the second-order fixed point in dependence on N for different approximations.
- Fig. 7: Values for e^2 and λ obtained with the φ^4 truncation and the global method for the tricritical fixed point in dependence on N . The solid line represents the large- N estimate given by eq. (40).
- Fig. 8: The critical index η as a function of N for two different approximations and in comparison with previous estimates.
- Fig. 9: The critical index ν as a function of N for two different approximations and in comparison with previous estimates.

Figure 1

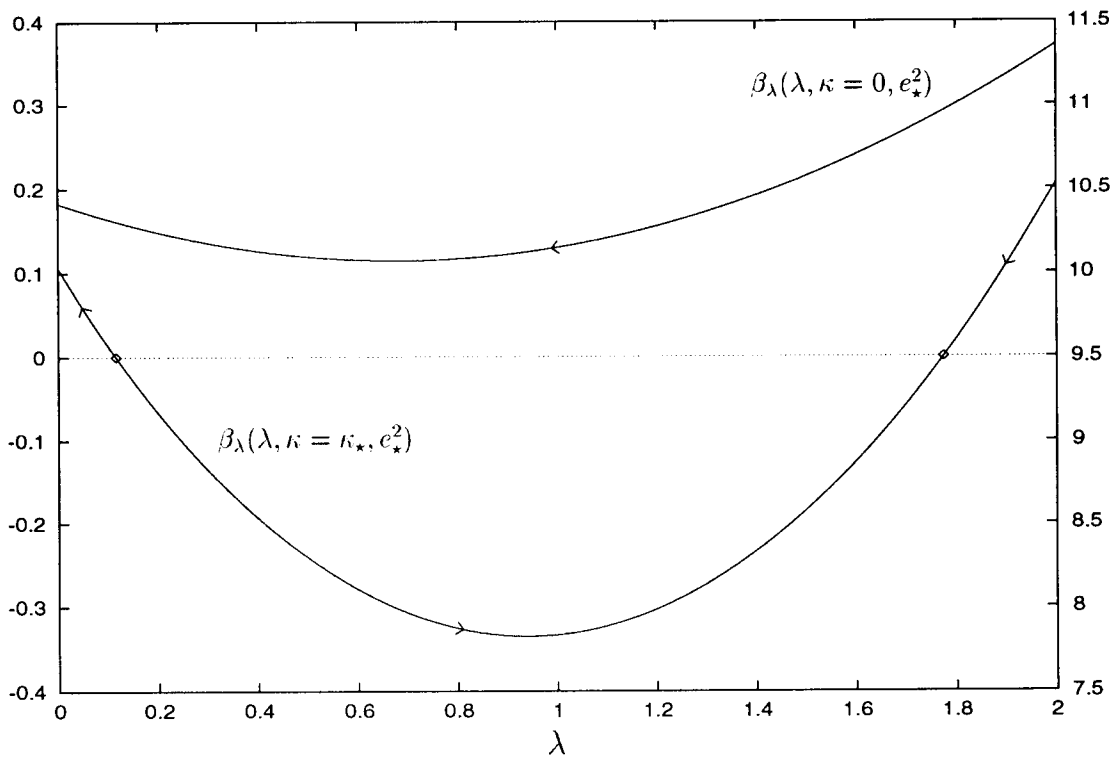


Figure 2

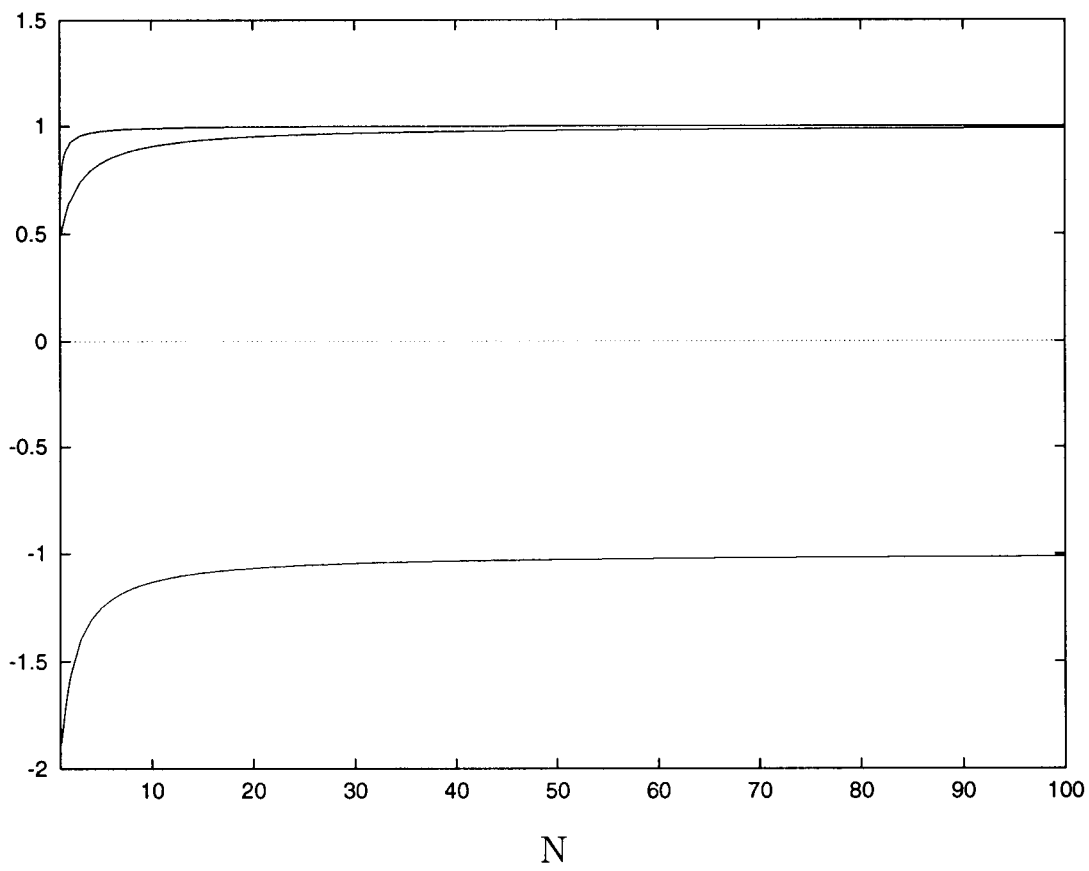


Figure 3

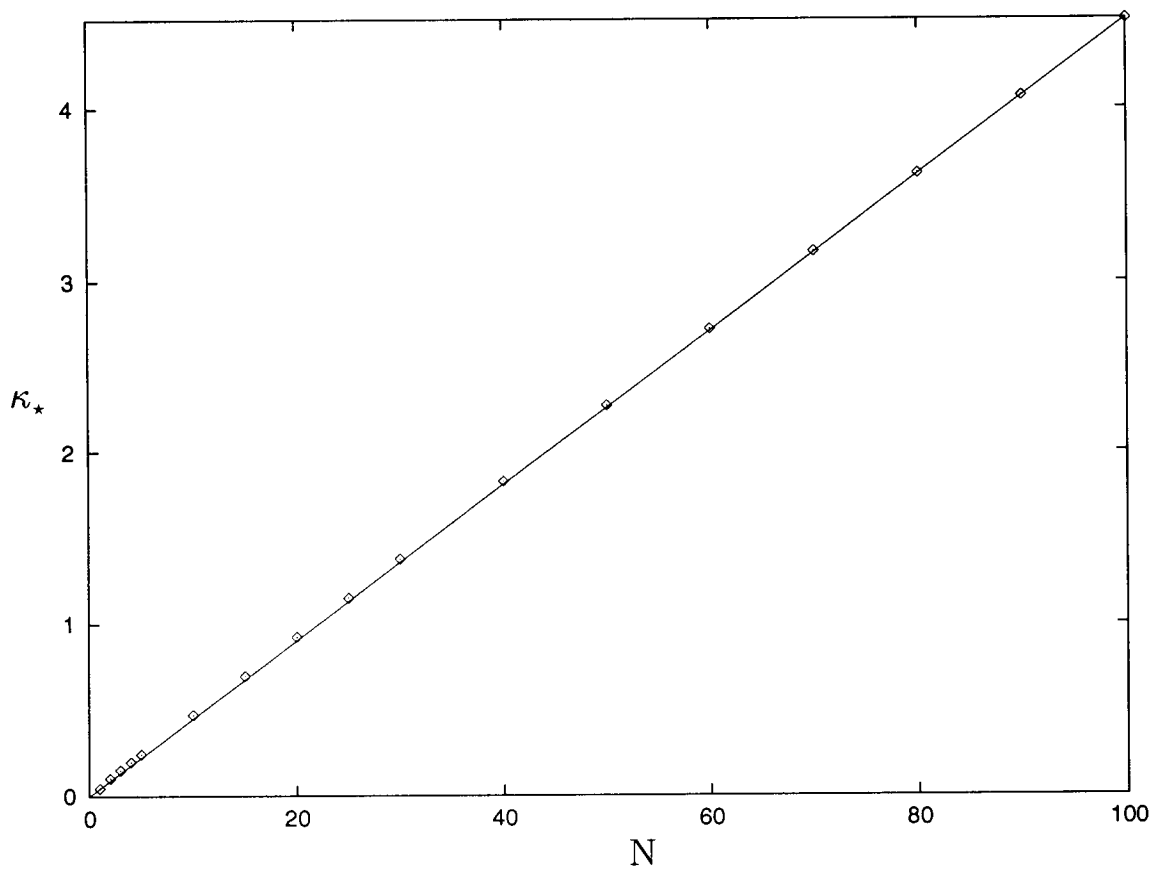


Figure 4

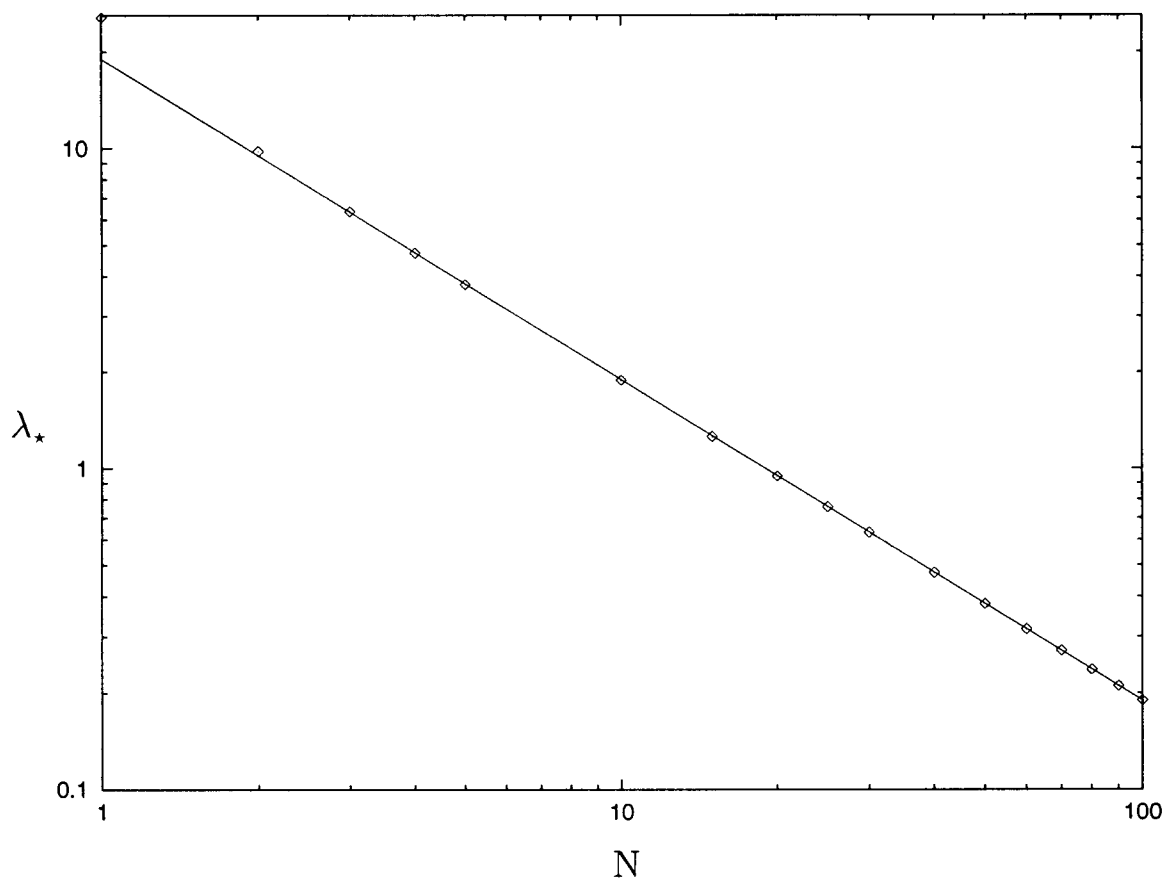


Figure 5

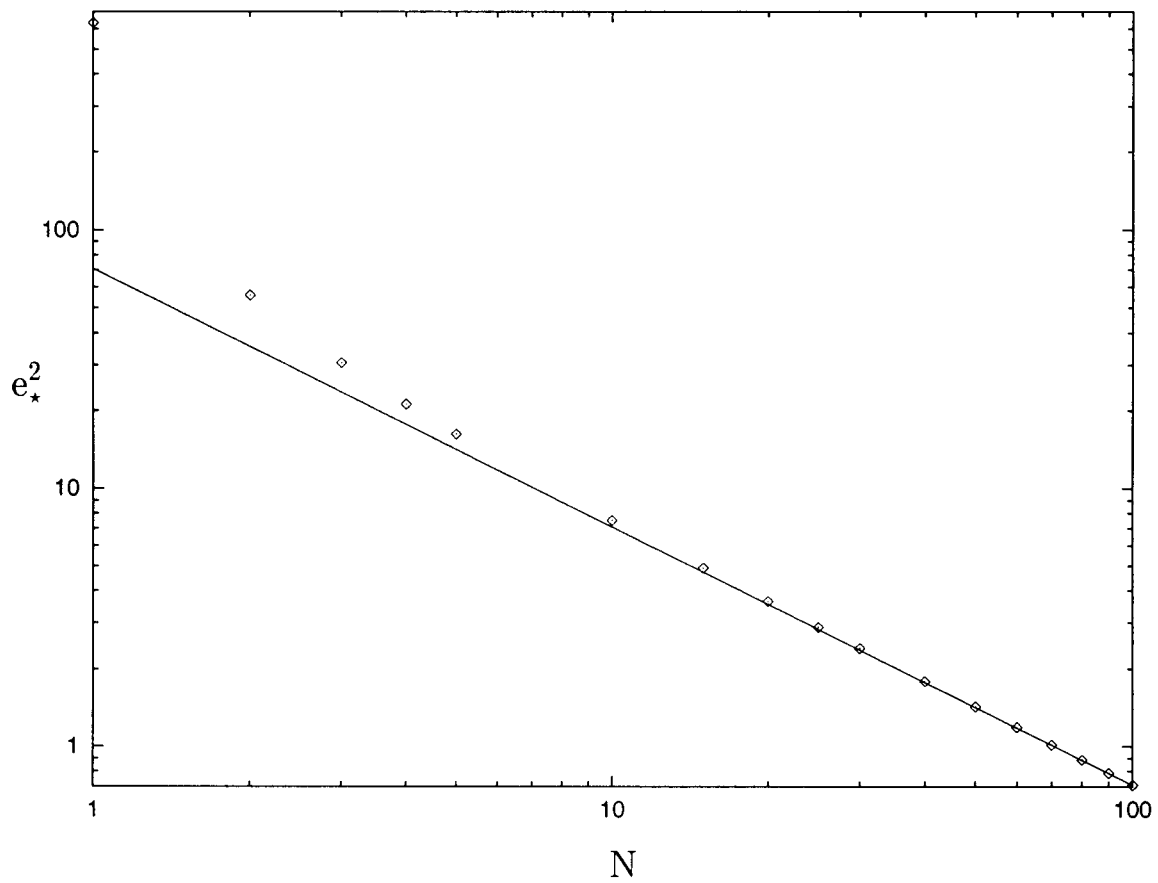


Figure 7

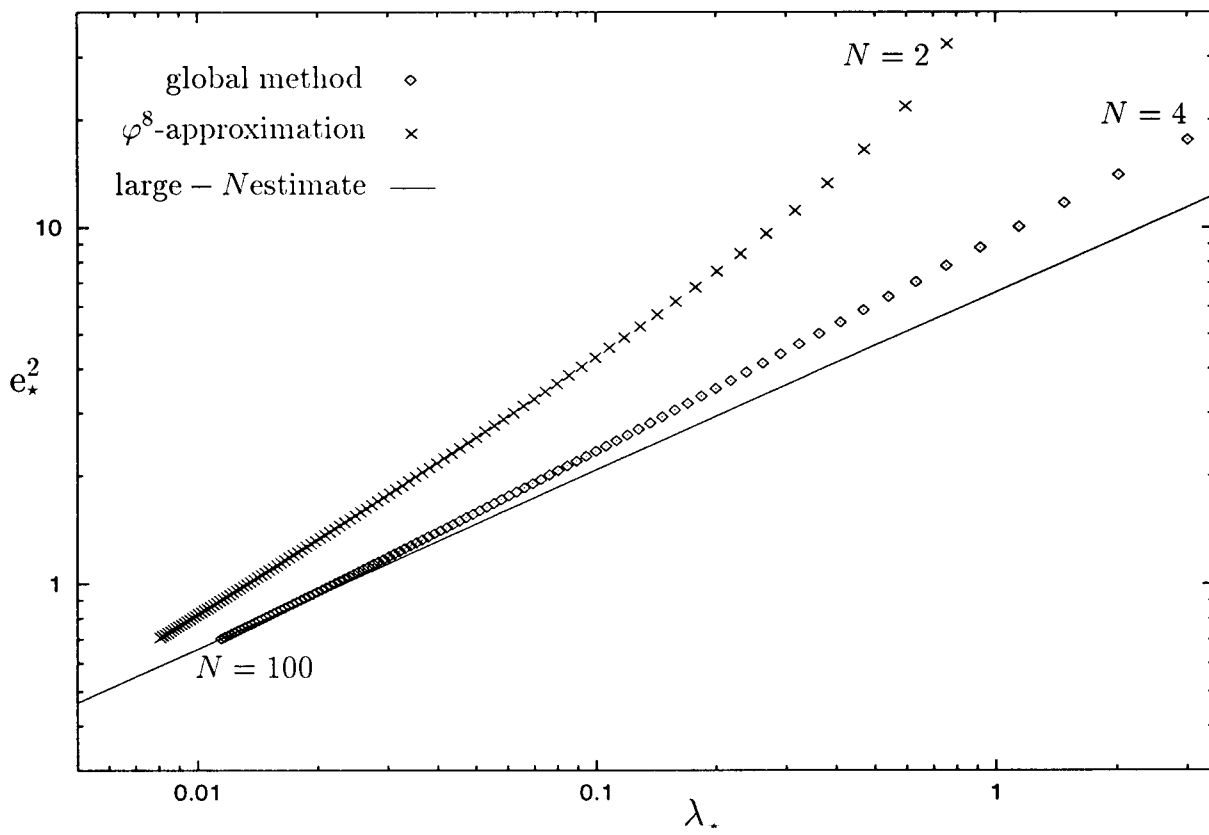


Figure 8

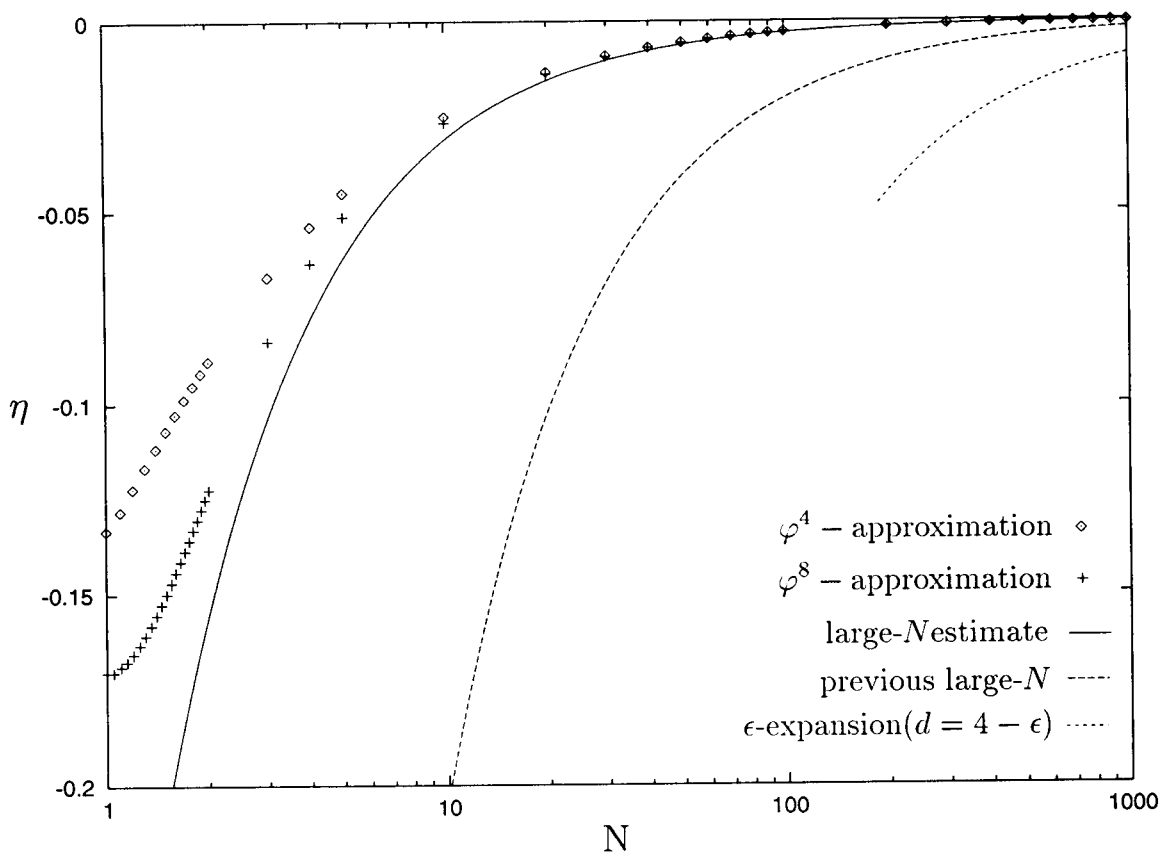


Figure 9

